Published in final edited form as:
Dev Biol. 2012 May 15; 365(2): 319–327. doi:10.1016/j.ydbio.2012.02.018.

Regulation of zebrafish heart regeneration by miR-133

Viravuth P. Yin[1,2], **Alexandra Lepilina**[1], **Ashley Smith**[2], and **Kenneth D. Poss**[1]

[1]Department of Cell Biology, Howard Hughes Medical Institute, Duke University Medical Center, Durham, NC 27710, USA

[2]Davis Center for Regenerative Biology and Medicine, Mount Desert Island Biological Labs, Salisbury Cove, ME 04672, USA

Abstract

Zebrafish regenerate cardiac muscle after severe injuries through the activation and proliferation of spared cardiomyocytes. Little is known about factors that control these events. Here we investigated the extent to which miRNAs regulate zebrafish heart regeneration. Microarray analysis identified many miRNAs with increased or reduced levels during regeneration. miR-133, a miRNA with known roles in cardiac development and disease, showed diminished expression during regeneration. Induced transgenic elevation of miR-133 levels after injury inhibited myocardial regeneration, while transgenic miR-133 depletion enhanced cardiomyocyte proliferation. Expression analyses indicated that cell cycle factors *mps1*, *cdc37*, and *PA2G4*, and cell junction components *cx43* and *cldn5*, are miR-133 targets during regeneration. With pharmacological inhibition and EGFP sensor interaction studies, we demonstrated that *cx43* is a new miR-133 target and regeneration gene. Our results reveal dynamic regulation of miRNAs during heart regeneration, and indicate that miR-133 restricts injury-induced cardiomyocyte proliferation.

Keywords

zebrafish; heart; regeneration; microRNAs; miR-133

Introduction

Recent evidence indicates that mammals possess a moderate capacity to renew cardiomyocytes (CMs) throughout postnatal life (Bergmann et al., 2009). Yet, there is little or no significant cardiac muscle regeneration after an injury like acute myocardial infarction. Adult zebrafish, on the other hand, robustly regenerate cardiac muscle after major injuries such as resection of the ventricular apex, surface cryoinjury, or genetic ablation of over 60% of CMs (Chablais et al., 2011; Gonzalez-Rosa et al., 2011; Poss et al., 2002b; Schnabel et al., 2011; Wang et al., 2011). Thus, dissecting successful heart regeneration in zebrafish can provide context for understanding, and possibly enhancing, mammalian cardiac regenerative capacity.

Corresponding author: Kenneth D. Poss, kenneth.poss@cellbio.duke.edu.

Author Contributions

V.P.Y. designed, generated and tested transgenic strains. V.P.Y. analyzed the miRNA and mRNA microarray datasets and performed validation experiments. V.P.Y. and A.L. executed the proliferation studies, *in situ* hybridizations and AFOG staining. A.S. conducted CBX drug treatments. V.P.Y. and K.D.P. designed the study and wrote the manuscript. All authors have read and approved the final version of this manuscript.

Disclosures

The authors have no disclosures to report.

Genetic lineage tracing studies recently revealed that existing CMs, not stem cells, are the major source of regenerating cardiac muscle in zebrafish (Jopling et al., 2010; Kikuchi et al., 2011a; Kikuchi et al., 2010). In response to injury, CMs induce cell cycle regulatory genes and proliferate to replace lost myocardium (Jopling et al., 2010; Kikuchi et al., 2010; Poss et al., 2002b). The cardiac environment created by non-muscle cells after injury is believed to be key in facilitating this regenerative response. Fibroblast growth factor and Platelet derived growth factor have been implicated in directing epicardial cells to the injury site, where they can influence muscle regeneration. Furthermore, retinoic acid (RA) synthesis localizes to epicardial cells and endocardial cells at the injury site, where RA signaling is required for CM proliferation (Kikuchi et al., 2011b), (Kim et al., 2010; Lepilina et al., 2006). It remains critical to define additional molecular regulators of injury-induced CM proliferation.

Previous studies of zebrafish heart regeneration have suggested that regenerating CMs acquire a less differentiated form after injury, with reduced contractile organization and altered electrical properties (Jopling et al., 2010; Kikuchi et al., 2010). Such a developmental transition suggests potential roles for microRNAs (miRNAs), small, noncoding RNAs that control many cellular processes by binding to mRNA target genes and inhibiting protein translation (He and Hannon, 2004). An abundance of studies have documented indispensable roles for miRNAs during embryonic development, homeostasis, and diseases including cardiomyopathy and cancer (Lin and Friedlander, 2010; Marquez et al., 2010; Sehm et al., 2009; Thatcher et al., 2008; Yin et al., 2008). With respect to tissue regeneration, it was shown recently that many miRNAs show dynamic regulation during fin regeneration and are involved in key regenerative signaling pathways mediated by Fibroblast growth factors and Wnts (Thatcher et al., 2008; Yin et al., 2008).

In this study, we used array analysis and new transgenic technology to investigate potential functions for miRNAs during heart regeneration. While many miRNAs showed differential regulation in regenerating versus uninjured cardiac tissue, we focused our work on miR-133, whose family members have been shown to regulate cardiac development and disease (Care et al., 2007; Liu et al., 2008). Our results indicate that miR-133 is an endogenous inhibitor of CM proliferation through modulation of *mps1* and *cx43* activity. Collectively, they support a model in which downregulation of miR-133 in CMs after injury contributes to the regenerative capacity of the zebrafish heart.

Materials and methods

Zebrafish and resection surgery

Zebrafish of the *Ekkwill* (EK) strain or EK/AB hybrid strain 4–6 months old were used for all experiments. Resection surgeries were performed with iridectomy scissors as previously described (Poss et al., 2002b). Transgenic strains were examined as heterozygotes and age-matched clutchmates were used as wildtype controls. For heat-shock experiments, transgenic *hsp70:miR-133*, *hsp70:miR-133sp* and wildtype clutchmates were heat-shocked from 26°C to 38°C at either the uninjured state, 6 days post-amputation (dpa), 29 dpa, or once daily for 29 days using experimental conditions previously described (Wills et al., 2008). Following the completion of heat treatment, fish were returned to 26°C aquaria and hearts were collected 24 hours later for analysis.

Gene expression analysis

Total RNA was isolated (Tri-Reagent, Sigma) from whole ventricles at the specified stages of regeneration and used for miRNA microarray hybridizations, Northern analysis, and quantitative PCR (Supplemental Methods; (Yin et al., 2008)).

miRNA and mRNA microarrays

Total RNA was isolated from 3 groups each of uninjured and 7 dpa ventricles for miRNA microarray hybridizations using miRBase v.13 miRNAs (www.lcsciences.com). Hybridizations and data filtration were performed by LCSciences in accordance to standard protocols. mRNA microarray hybridizations were performed in triplicate with total RNA isolated from wildtype, *hsp70:miR-133* and *hsp70:miR-133sp* ventricles 5 hours following the completion of heat-treatment. MoGene Services performed RNA labeling and hybridizations onto NimbleGene oligo arrays (www.NimbleGen, www.MoGene.com).

Histological methods

Zebrafish hearts were extracted and fixed in 4% paraformaldehyde (PFA) at room temperature for 1 hr. Histological analyses were performed on 10 μm cryosections as previously described (Kikuchi et al., 2011b). Immunofluorescence, *in situ* hybridization, and Acid Fuchsin Orange G stains (detecting fibrin and collagen) were performed as described previously (Kikuchi et al., 2011b) and images were captured at 20× using Olympus BX53 microscope and Retiga 2000DC camera. Primary antibodies used in this study were: anti-Mef2 (rabbit; Santa Cruz Biotechnology), anti-PCNA (Sigma), Alexa Fluor 594 goat anti-rabbit IgG (H+L) for anti-Mef2 and Alexa Fluor594 goat anti-mouse IgG (H+L) for anti-PCNA (Invitrogen). To quantify cardiomyocyte proliferation, three sections showing the largest wounds were selected from each heart. The number of $Mef2^+$ and $Mef2^+PCNA^+$ cells within a defined region of 230 pixels (in vertical) was manually counted. To establish a CM proliferation index, an average of $Mef2^+PCNA^+$ cells were represented over the total number of Mef2+ cells, for each heart. Each experiment had at least 10 hearts per group. In situ hybridizations for miR-133 were performed with 3' DIG labelled LNA antisense oligonucleotides in accordance using established protocols (Kloosterman et al., 2006).

Results

Differential regulation of miRNAs during heart regeneration

To investigate potential contributions of miRNAs during zebrafish heart regeneration, we employed microarrays and real-time quantitative PCR (Q-PCR) to identify miRNAs that are differentially regulated after resection of the ventricular apex. We compared miRNA expression levels between uninjured and regenerating ventricles at 7 days post amputation (dpa), and identified 10 miRNAs that were significantly elevated during cardiac regeneration (Fig. 1A, 1B). Conversely, this analysis also revealed 8 miRNAs with diminished expression after resection (Fig. 1A, 1B). Interestingly, many of the miRNAs that we identified in our regeneration model were shown also to be modulated in transverse aortic banding (TAB) and coronary ligation studies in mice, including miR-17a, miR-21, miR-92, miR-146a, miR-150, miR-210 and miR-133 (Fig. 1A, 1B (Liu et al., 2008; Matkovich et al., 2010; Sayed et al., 2007; Small et al., 2010; Thum et al., 2008; Yu and Li, 2010)). Thus, miRNAs are dynamically controlled after cardiac injury in zebrafish, suggesting that they might contribute to key regenerative events.

The cardiomyocyte miRNA miR-133 is diminished during regeneration

To ascertain the contributions of miRNAs during heart regeneration, we focused on the CM-specific miR-133. Previous work on mammalian miR-133 revealed an indispensable role for CM proliferation and ventricular septation during embryonic cardiac development (Liu et al., 2008). Also, antisense antagonism of miR-133 caused pathologic hypertrophy in adult mice (Care et al., 2007). We found that miR-133 levels were decreased at 7 dpa from levels of uninjured ventricles, but returned to baseline by 30–60 dpa, a stage when myocardial regeneration is normally completed (Fig. 1C). Zebrafish possess 4 miR-133 family

members, miR-133a1, -a2, 133b and miR-133c, differing at most by 2 nucleotides in the 3' region of the mature species. miR-133 is a highly conserved muscle miRNA and alignment between the mouse and zebrafish revealed that the mature miR-133a sequence is identical. In situ hybridization indicated that miR-133a is restricted to CMs at all timepoints (Fig. 1D, 1E). These studies indicated that CM miR-133 is diminished in response to cardiac injury, similar to what has been reported during mammalian cardiac hypertrophy (Care et al., 2007).

Transgenic modulation of miR-133 during heart regeneration

To determine the impact of changes in miR-133 levels during regeneration, we generated two new transgenic reagents enabling overexpression or depletion of miR-133 (Fig. 2A). To increase miR-133 levels, we generated a transgenic strain containing ~250 bp of genomic sequences flanking both sides of the miR-133a1 precursor sequence, downstream of a heat shock-inducible *hsp70* promoter (*Tg(hsp70:miR-133a1)*^{pd47}; Fig. 2A, top), referred to as *hsp70:miR-133*. To assess the activation and processing of mature miR-133, we subjected wildtype and *hsp70:miR-133* adults to a single heat-treatment at 38°C and performed expression studies. We detected a ~1.8-fold increase of mature miR-133 in *hsp70:miR-133* animals over wildtype levels, both in uninjured and 7 dpa ventricles via Northern blot hybridizations and real-time quantitative PCR (Fig. 2B, 2F). As in mammals, zebrafish miR-133a1 is transcribed in tandem with miR-1 on a single transcript separated by ~2.2-kb of genomic sequence (www.mirbase.org). miR-133 overexpression in the *hsp70:miR-133* strain had no gross effects on miR-1 transcription or maturation (Fig. 2B).

To reduce miR-133 levels during heart regeneration, we engineered a miR-133 "sponge" construct, encoding a *EGFP* cDNA followed by triplicate perfect binding sites for miR-133 (Fig. 2A, bottom). Based on similar strategies in other systems, we predicted that expression of this construct would lead to binding and depletion of endogenous miR-133 levels (Ebert et al., 2007; Loya et al., 2009). This construct was placed downstream of the *hsp70* promoter, and *Tg(hsp70:miR-133sp)*^{pd48}, referred to as (*hsp70:miR-133sp*), transgenic lines were generated. Remarkably, a single heat shock was sufficient to knock down adult cardiac miR-133 expression to near undetectable amounts for 24 hours (Fig. 2B–2F). Northern blot studies, in situ hybridizations and Q-PCR assays all confirm the depletion of miR-133 with *hsp70:miR-133sp* activation. We also examined expression of additional cardiac miRNAs under conditions of miR-133 elevation or depletion, and saw no gross changes in levels of miR-1, miR-21, miR-24, miR-29, miR-144, miR-181 and miR-182 (Fig. 2F). Thus, these new inducible overexpression strains enabled examination of specific miRNA functions during heart regeneration.

miR-133 restricts CM proliferation during heart regeneration

To define contributions of miR-133 during heart regeneration, we modulated miR-133 activity with a single heat shock 6 days after resection injury and examined CM proliferation, a key metric for cardiac regeneration, one day later (Fig. 3A, 3I). We stained heart sections with antibodies directed against Mef2 (Fig. 3A–3C), to detect CMs, and with PCNA (Fig. 3D–3F), as an indicator of proliferation. To obtain CM proliferation indices, we determined the number of $Mef2^{+}PCNA^{+}$ cells as a percentage of the total population of CMs within a defined region. While wildtype controls had a CM proliferation index of 14.5% at 7 dpa, elevation of miR-133 levels with the *hsp70:miR-133* strain reduced CM proliferation by ~45% to 8.0%. Conversely, depleting miR-133 with the *hsp70:miR-133sp* transgenic reagent increased CM proliferation index by ~40% to 20.4% (Fig. 3J). CM proliferation was largely restricted to cells near the injury during miR-133 depletion, and *hsp70:miR-133sp* induction did not increase CM proliferation in uninjured ventricles (Fig. 3J). This suggests that miR-133 reduction is permissive rather than instructive during cardiac regeneration.

Collectively, these data indicate that miR-133 expression negatively influences CM proliferation.

Given that increases or decreases in miR-133 levels over a one-day period were sufficient to modify CM proliferation, we asked how cardiac regeneration might be impacted by long-term modulation of miR-133 levels. Following partial ventricular resection, wildtype, *hsp70:miR-133* and *hsp70:miR-133sp* animals were given daily 38°C heat shocks for a duration of 30 days. Surprisingly, continued depletion of miR-133 elevated CM proliferation at 30 dpa from 0.8% to ~6%, a timepoint when a new myocardial wall has typically been restored (Fig. 4A–4C, 4G), an effect that was not seen after a single heat shock at 30 dpa (Fig. 4G). Conversely, heat-treated *hsp70:miR-133* animals displayed gaps in the myocardial wall after 30 days of sustained heat-shock, indicative of poor regeneration (Fig. 4B, 4E). To determine if scars formed during these events, we stained ventricles for collagen. Prominent scar tissue was observed in each of the 30 dpa samples (n = 10/10), contrasting with wildtype (n = 0/10) and *hsp70:miR-133sp* hearts (n = 1/10) (Fig. 4D–4F). These results indicate that miR-133 presence is an impediment to cardiac regeneration, leading to scarring as an alternative repair process. Interestingly, accentuating depletion of miR-133 had the effects of enhancing the regenerative response of CMs.

Targets of miR-133 during heart regeneration

To determine the cardiac targets of miR-133, we performed microarray analysis on 7 dpa wildtype control, *hsp70:miR-133* and *hsp70:miR-133sp* hearts collected 5 hours after a single heat shock. As miRNAs typically downregulate target genes, we filtered our data for genes that displayed at least a 1.5-fold upregulation in the *hsp70:miR-133sp* samples, and a 1.5-fold downregulation in *hsp70:miR-133* samples as compared with wildtypes. These analyses revealed 1422 genes elevated in *hsp70:miR-133sp* samples and 1044 genes reduced in *hsp70:miR-133* samples (Fig. 5A, 5B). We reasoned that potential miR-133 target genes are likely to be represented in both datasets, and identified 170 genes that were present in both groups (Fig. 5C). Many of these potential target genes fell into one of three major categories of biological processes: energy homeostasis and metabolism, cytoskeletal/structural components, and cell cycle regulators (Supplemental Table 1).

We queried this list of potential target genes for factors predicted to harbor miR-133 binding sites and likely to be involved in tissue regeneration or cardiac function, using the Microcosm database. Q-PCR confirmed that the cell cycle regulators *B-cell translocation gene 3 (btg3), cell division cycle 37 (cdc37)*, *proliferation associated protein* (PA2G4) and *monopolar spindle 1* (*mps1)*, each displayed inverse expression changes with miR-133 manipulation (Fig. 5D). Interestingly, *mps1* had previously been identified as an essential factor for zebrafish heart regeneration (Poss et al., 2002b). In addition to this class of genes, cytoskeletal/structural component proteins *myosin IC (myoc1), protocadherin 15a (pcdh15a), connexin-43* (*cx43)* and *claudin-5 (cldn5)* had increased expression with transgenic miR-133 depletion and reduced expression with miR-133 elevation (Fig. 5D). The junction proteins, *cx43* and *cldn5* are implicated in human cardiomyopathies (Bruce et al., 2008; Formigli et al., 2003; Kostin et al., 2004; Mays et al., 2008; Sanford et al., 2005). To interpret the possible effects of *cx43* downregulation by miR-133 during regeneration, we resected ventricles and allowed regeneration to proceed for 6 days, exposed adult zebrafish for 24 hours to 50 μM carbenoxolone (CBX), an inhibitor of Cx43 (Song et al., 2009), and stained for Mef2 and PCNA. Pharmacological inhibition of Cx43 from 6 to 7 dpa reduced the CM proliferation index by 55% (6.2%, n = 14) compared to vehicle-treated animals (13.8%, n = 11) (Fig. 6A–6C). These data indicate that regulatory effects of miR-133 on CM proliferation are mediated in part through *mps1* and *cx43* regulation.

To examine *in vivo* miR-133 regulation of *cx43* expression, we performed an embryo EGFP sensor study (Flynt et al., 2007; Giraldez et al., 2005; Yin et al., 2008). We injected a sensor mRNA construct consisting of EGFP fused to the predicted miR-133 binding site within the *cx43* 3' UTR into 1-cell zebrafish embryos, in the presence or absence of miR-133 RNA duplex. One day later, we quantified EGFP fluorescence as an indicator of Cx43 expression. While *EGFP-cx43* sensor mRNA alone resulted in high EGFP fluorescence, this signal was reduced ~41% by co-injection of miR-133 RNA duplex (Fig. 6D, 6E). Importantly, miR-133 duplex had negligible effects on expression by a *EGFP-cx43* sensor mRNA with point mutations in the miR-133 binding site (Fig. 6D–6F). In summary, these findings implicate *cx43* as a new miR-133 target and key regeneration gene.

Discussion

miRNAs are intriguing candidates to regulate cardiac regeneration, given their ability to simultaneously influence many different mRNA targets. Here, we investigated their involvement in adult zebrafish, a model system with high cardiac regenerative capacity. We found that several miRNAs were dynamically regulated after cardiac injury, and we engineered inducible transgenic reagents to modulate and define the importance of miR-133. miR-133 levels normally decrease after injury, and our data indicate that it functions at least in part by restricting CM proliferation. Increasing miR-133 levels favored scarring over regeneration, while depletion of miR-133 levels enhanced CM proliferation even beyond the normally robust response. This genetic manipulation is unprecedented in its ability to enhance cardiac regenerative responses in zebrafish, and indicates that miR-133 depletion which normally occurs in zebrafish CMs after injury is important for cardiac regenerative capacity.

Multiple studies have shown that miRNAs play prominent roles in mediating cellular stress responses (Leung and Sharp, 2007). Moreover, previous work investigating cardiac miR-208 function revealed phenotypes only when animals were challenged in pressure overload studies (van Rooij et al., 2007). In our study, we noted that CM proliferation was not significantly affected in the absence of cardiac injury, irrespective of miR-133 expression levels. Thus, the impact of miR-133 may be similarly limited in the absence of trauma.

Our observations of miR-133 function during heart regeneration provide new context for understanding roles of miR-133 in CM biology. In a previous report, genetic knockout of miR-133a1/a2 elevated CM proliferation in neonatal mice (Liu et al., 2008), consistent with the role we identify with miR-133 during zebrafish heart regeneration. Additionally, a study of pathological cardiac hypertrophy in adult mice indicated that miR-133 levels decrease during cardiac hypertrophy, and that miR-133 inhibits disease progression (Care et al., 2007). It is possible that the hyperplastic response to cardiac injury in adult zebrafish is evolutionarily related to hypertrophy in mammals, and that miR-133 reduction is a remnant shared by bothregeneration and disease.

Potentially different functions of miR-133 during development and regeneration versus disease might also reflect target gene regulation. Our results predicted several target genes during heart regeneration based on 3' UTR sequence complementarity and expression profiles. One of these genes, *mps1*, is not only essential for heart regeneration, but is critical for fin regeneration and was identified as an miR-133 target gene during this process as well (Poss et al., 2002a; Yin et al., 2008). That the miR-133-*mps1* regulatory unit is present in two different regenerative contexts suggests that this circuit may be generally advantageous for tissue regeneration. Other implicated target genes encode the cell junction proteins Cld5 and Cx43, the latter of which we found has activity required for normal regenerative responses to cardiac injury. This finding might reflect a key role for intercellular molecular

exchange during regeneration; indeed, recent studies have implicated gap junctions during planarian body regeneration and sodium ions during amphibian appendage regeneration (Oviedo and Levin, 2007; Oviedo et al., 2010; Tseng et al., 2010). Because of potential influences on key events like CM proliferation, miRNAs such as miR-133 represent attractive targets for enhancing the regenerative capacity of the injured mammalian heart.

Supplementary Material

Refer to Web version on PubMed Central for supplementary material.

Acknowledgments

We thank J. Burris and A. Eastes for excellent zebrafish care, and J. Coffman, K. Strange, and G. Nachtrab for critical comments on this manuscript. V.P.Y. was supported by an American Heart Association post-doctoral fellowship. K.D.P. is an Early Career Scientist of the Howard Hughes Medical Institute. This work was supported by grants 5P20-RR016463 from NCRR (V.P.Y) and (8 P20 GM103423-12) from NIGMS (V.P.Y), R01-HL081674 from NHLBI (K.D.P.) and the Pew Charitable Trusts (K.D.P.).

References

Bergmann O, Bhardwaj RD, Bernard S, Zdunek S, Barnabe-Heider F, Walsh S, Zupicich J, Alkass K, Buchholz BA, Druid H, Jovinge S, Frisen J. Evidence for cardiomyocyte renewal in humans. Science (New York, NY. 2009; 324:98–102.

Bruce AF, Rothery S, Dupont E, Severs NJ. Gap junction remodelling in human heart failure is associated with increased interaction of connexin43 with ZO-1. Cardiovasc Res. 2008; 77:757–765. [PubMed: 18056766]

Care A, Catalucci D, Felicetti F, Bonci D, Addario A, Gallo P, Bang ML, Segnalini P, Gu Y, Dalton ND, Elia L, Latronico MV, Hoydal M, Autore C, Russo MA, Dorn GW 2nd, Ellingsen O, Ruiz-Lozano P, Peterson KL, Croce CM, Peschle C, Condorelli G. MicroRNA-133 controls cardiac hypertrophy. Nat Med. 2007; 13:613–618. [PubMed: 17468766]

Chablais F, Veit J, Rainer G, Jazwinska A. The zebrafish heart regenerates after cryoinjury-induced myocardial infarction. BMC Dev Biol. 2011; 11:21. [PubMed: 21473762]

Ebert MS, Neilson JR, Sharp PA. MicroRNA sponges: competitive inhibitors of small RNAs in mammalian cells. Nature methods. 2007; 4:721–726. [PubMed: 17694064]

Flynt AS, Li N, Thatcher EJ, Solnica-Krezel L, Patton JG. Zebrafish miR-214 modulates Hedgehog signaling to specify muscle cell fate. Nat Genet. 2007; 39:259–263. [PubMed: 17220889]

Formigli L, Ibba-Manneschi L, Perna AM, Pacini A, Polidori L, Nediani C, Modesti PA, Nosi D, Tani A, Celli A, Neri-Serneri GG, Quercioli F, Zecchi-Orlandini S. Altered Cx43 expression during myocardial adaptation to acute and chronic volume overloading. Histol Histopathol. 2003; 18:359–369. [PubMed: 12647785]

Giraldez AJ, Cinalli RM, Glasner ME, Enright AJ, Thomson JM, Baskerville S, Hammond SM, Bartel DP, Schier AF. MicroRNAs regulate brain morphogenesis in zebrafish. Science. 2005; 308:833–838. [PubMed: 15774722]

Gonzalez-Rosa JM, Martin V, Peralta M, Torres M, Mercader N. Extensive scar formation and regression during heart regeneration after cryoinjury in zebrafish. Development. 2011; 138:1663–1674. [PubMed: 21429987]

He L, Hannon GJ. MicroRNAs: small RNAs with a big role in gene regulation. Nat Rev Genet. 2004; 5:522–531. [PubMed: 15211354]

Jopling C, Sleep E, Raya M, Marti M, Raya A, Belmonte JC. Zebrafish heart regeneration occurs by cardiomyocyte dedifferentiation and proliferation. Nature. 2010; 464:606–609. [PubMed: 20336145]

Kedersha N, Stoecklin G, Ayodele M, Yacono P, Lykke-Andersen J, Fritzler MJ, Scheuner D, Kaufman RJ, Golan DE, Anderson P. Stress granules and processing bodies are dynamically linked sites of mRNP remodeling. J Cell Biol. 2005; 169:871–884. [PubMed: 15967811]

Kikuchi K, Gupta V, Wang J, Holdway JE, Wills AA, Fang Y, Poss KD. tcf21+ epicardial cells adopt non-myocardial fates during zebrafish heart development and regeneration. Development. 2011a; 138:2895–2902. [PubMed: 21653610]

Kikuchi K, Holdway JE, Major RJ, Blum N, Dahn RD, Begemann G, Poss KD. Retinoic acid production by endocardium and epicardium is an injury response essential for zebrafish heart regeneration. Dev Cell. 2011b; 20:397–404. [PubMed: 21397850]

Kikuchi K, Holdway JE, Werdich AA, Anderson RM, Fang Y, Egnaczyk GF, Evans T, Macrae CA, Stainier DY, Poss KD. Primary contribution to zebrafish heart regeneration by gata4(+) cardiomyocytes. Nature. 2010; 464:601–605. [PubMed: 20336144]

Kim J, Wu Q, Zhang Y, Wiens KM, Huang Y, Rubin N, Shimada H, Handin RI, Chao MY, Tuan TL, Starnes VA, Lien CL. PDGF signaling is required for epicardial function and blood vessel formation in regenerating zebrafish hearts. Proceedings of the National Academy of Sciences of the United States of America. 2010; 107:17206–17210. [PubMed: 20858732]

Kloosterman WP, Wienholds E, de Bruijn E, Kauppinen S, Plasterk RH. In situ detection of miRNAs in animal embryos using LNA-modified oligonucleotide probes. Nat Methods. 2006; 3:27–29. [PubMed: 16369549]

Kostin S, Dammer S, Hein S, Klovekorn WP, Bauer EP, Schaper J. Connexin 43 expression and distribution in compensated and decompensated cardiac hypertrophy in patients with aortic stenosis. Cardiovasc Res. 2004; 62:426–436. [PubMed: 15094362]

Lepilina A, Coon AN, Kikuchi K, Holdway JE, Roberts RW, Burns CG, Poss KD. A dynamic epicardial injury response supports progenitor cell activity during zebrafish heart regeneration. Cell. 2006; 127:607–619. [PubMed: 17081981]

Leung AK, Calabrese JM, Sharp PA. Quantitative analysis of Argonaute protein reveals microRNA-dependent localization to stress granules. Proc Natl Acad Sci U S A. 2006; 103:18125–18130. [PubMed: 17116888]

Leung AK, Sharp PA. microRNAs: a safeguard against turmoil? Cell. 2007; 130:581–585. [PubMed: 17719533]

Lin N, Friedlander RM. Regeneration of neuromuscular synapses: action of microRNA-206. Neurosurgery. 2010; 66:N19–20. [PubMed: 20305481]

Liu N, Bezprozvannaya S, Williams AH, Qi X, Richardson JA, Bassel-Duby R, Olson EN. microRNA-133a regulates cardiomyocyte proliferation and suppresses smooth muscle gene expression in the heart. Genes & development. 2008; 22:3242–3254. [PubMed: 19015276]

Loya CM, Lu CS, Van Vactor D, Fulga TA. Transgenic microRNA inhibition with spatiotemporal specificity in intact organisms. Nat Methods. 2009; 6:897–903. [PubMed: 19915559]

Marquez RT, Wendlandt E, Galle CS, Keck K, McCaffrey AP. MicroRNA-21 is upregulated during the proliferative phase of liver regeneration, targets Pellino-1, and inhibits NF-kappaB signaling. Am J Physiol Gastrointest Liver Physiol. 2010; 298:G535–541. [PubMed: 20167875]

Matkovich SJ, Wang W, Tu Y, Eschenbacher WH, Dorn LE, Condorelli G, Diwan A, Nerbonne JM, Dorn GW 2nd. MicroRNA-133a protects against myocardial fibrosis and modulates electrical repolarization without affecting hypertrophy in pressure-overloaded adult hearts. Circ Res. 2010; 106:166–175. [PubMed: 19893015]

Mays TA, Binkley PF, Lesinski A, Doshi AA, Quaile MP, Margulies KB, Janssen PM, Rafael-Fortney JA. Claudin-5 levels are reduced in human end-stage cardiomyopathy. J Mol Cell Cardiol. 2008; 45:81–87. [PubMed: 18513742]

Oviedo NJ, Levin M. smedinx-11 is a planarian stem cell gap junction gene required for regeneration and homeostasis. Development (Cambridge, England). 2007; 134:3121–3131.

Oviedo NJ, Morokuma J, Walentek P, Kema IP, Gu MB, Ahn JM, Hwang JS, Gojobori T, Levin M. Long-range neural and gap junction protein-mediated cues control polarity during planarian regeneration. Developmental biology. 2010; 339:188–199. [PubMed: 20026026]

Poss KD, Nechiporuk A, Hillam AM, Johnson SL, Keating MT. Mps1 defines a proximal blastemal proliferative compartment essential for zebrafish fin regeneration. Development. 2002a; 129:5141–5149. [PubMed: 12399306]

Poss KD, Wilson LG, Keating MT. Heart regeneration in zebrafish. Science. 2002b; 298:2188–2190. [PubMed: 12481136]

Sanford JL, Edwards JD, Mays TA, Gong B, Merriam AP, Rafael-Fortney JA. Claudin-5 localizes to the lateral membranes of cardiomyocytes and is altered in utrophin/dystrophin-deficient cardiomyopathic mice. J Mol Cell Cardiol. 2005; 38:323–332. [PubMed: 15698839]

Sayed D, Hong C, Chen IY, Lypowy J, Abdellatif M. MicroRNAs play an essential role in the development of cardiac hypertrophy. Circ Res. 2007; 100:416–424. [PubMed: 17234972]

Schnabel K, Wu CC, Kurth T, Weidinger G. Regeneration of cryoinjury induced necrotic heart lesions in zebrafish is associated with epicardial activation and cardiomyocyte proliferation. PLoS One. 2011; 6:e18503. [PubMed: 21533269]

Sehm T, Sachse C, Frenzel C, Echeverri K. miR-196 is an essential early-stage regulator of tail regeneration, upstream of key spinal cord patterning events. Dev Biol. 2009; 334:468–480. [PubMed: 19682983]

Small EM, Frost RJ, Olson EN. MicroRNAs add a new dimension to cardiovascular disease. Circulation. 2010; 121:1022–1032. [PubMed: 20194875]

Song M, Yu X, Cui X, Zhu G, Zhao G, Chen J, Huang L. Blockade of connexin 43 hemichannels reduces neointima formation after vascular injury by inhibiting proliferation and phenotypic modulation of smooth muscle cells. Exp Biol Med (Maywood). 2009; 234:1192–1200. [PubMed: 19596827]

Thatcher EJ, Paydar I, Anderson KK, Patton JG. Regulation of zebrafish fin regeneration by microRNAs. Proc Natl Acad Sci U S A. 2008; 105:18384–18389. [PubMed: 19015519]

Thum T, Gross C, Fiedler J, Fischer T, Kissler S, Bussen M, Galuppo P, Just S, Rottbauer W, Frantz S, Castoldi M, Soutschek J, Koteliansky V, Rosenwald A, Basson MA, Licht JD, Pena JT, Rouhanifard SH, Muckenthaler MU, Tuschl T, Martin GR, Bauersachs J, Engelhardt S. MicroRNA-21 contributes to myocardial disease by stimulating MAP kinase signalling in fibroblasts. Nature. 2008; 456:980–984. [PubMed: 19043405]

Tseng AS, Beane WS, Lemire JM, Masi A, Levin M. Induction of vertebrate regeneration by a transient sodium current. The Journal of neuroscience : the official journal of the Society for Neuroscience. 2010; 30:13192–13200. [PubMed: 20881138]

van Rooij E, Sutherland LB, Qi X, Richardson JA, Hill J, Olson EN. Control of stress-dependent cardiac growth and gene expression by a microRNA. Science. 2007; 316:575–579. [PubMed: 17379774]

Wang J, Panakova D, Kikuchi K, Holdway JE, Gemberling M, Burris JS, Singh SP, Dickson AL, Lin YF, Sabeh MK, Werdich AA, Yelon D, Macrae CA, Poss KD. The regenerative capacity of zebrafish reverses cardiac failure caused by genetic cardiomyocyte depletion. Development. 2011; 138:3421–3430. [PubMed: 21752928]

Wills AA, Holdway JE, Major RJ, Poss KD. Regulated addition of new myocardial and epicardial cells fosters homeostatic cardiac growth and maintenance in adult zebrafish. Development. 2008; 135:183–192. [PubMed: 18045840]

Yin VP, Thomson JM, Thummel R, Hyde DR, Hammond SM, Poss KD. Fgf-dependent depletion of microRNA-133 promotes appendage regeneration in zebrafish. Genes Dev. 2008; 22:728–733. [PubMed: 18347091]

Yu S, Li G. MicroRNA expression and function in cardiac ischemic injury. J Cardiovasc Transl Res. 2010; 3:241–245. [PubMed: 20535240]

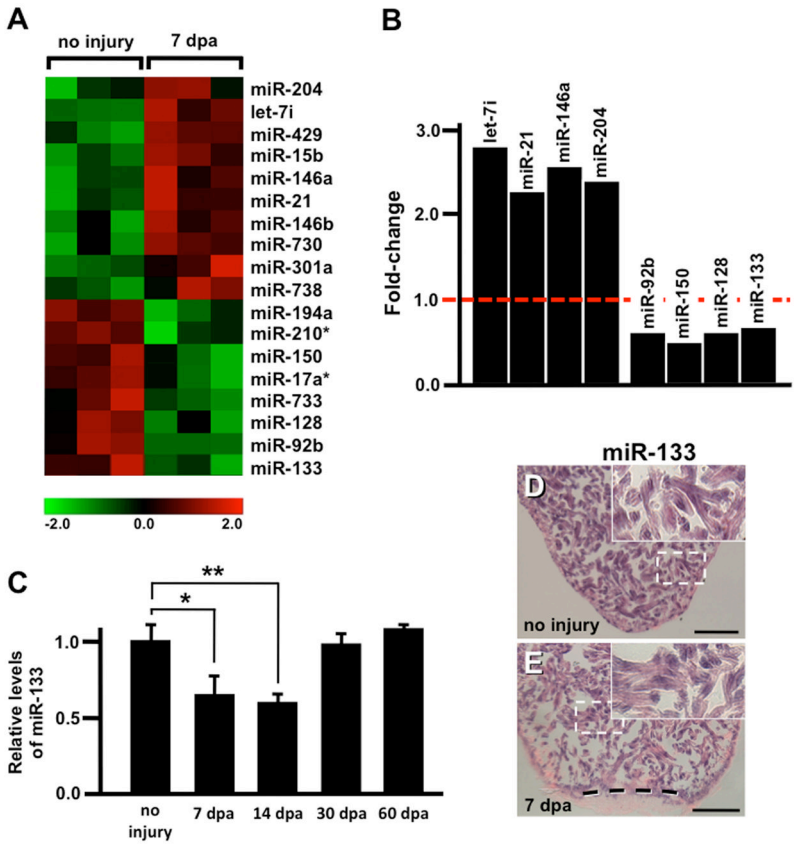

Fig. 1.

miRNAs are dynamically regulated during myocardial regeneration. A) A heat-map depicts triplicate microarray hybridizations, revealing a subset of miRNAs that are differentially expressed at 7 dpa when compared to uninjured samples. (Green) lower expression; (red) higher expression. B) Real-time quantitative PCR (QPCR) studies confirm the upregulation of let-7i, miR-21, miR-146A and miR-204 and downregulation of miR-92b, miR-150, miR-128 and miR-133 at 7 dpa when compared to uninjured samples. C) QPCR studies show miR-133 levels are high in the uninjured adult heart and reduced at 7 dpa. Levels return to near uninjured levels by 30–60 dpa. D–E) *In situ* hybridizations reveal miR-133 is restricted to cardiomyocytes under conditions of no injury and at 7 dpa. Error bars in (C) represent SEM, Student's t-test p-value <0.05 for * and **; Inserts in (D–E), high zoom images of the white dashed rectangle; Dashed line in (E) represents approximate amputation plane; dpa, days post-amputation; scale bar in (D–E) represents 100 μm.

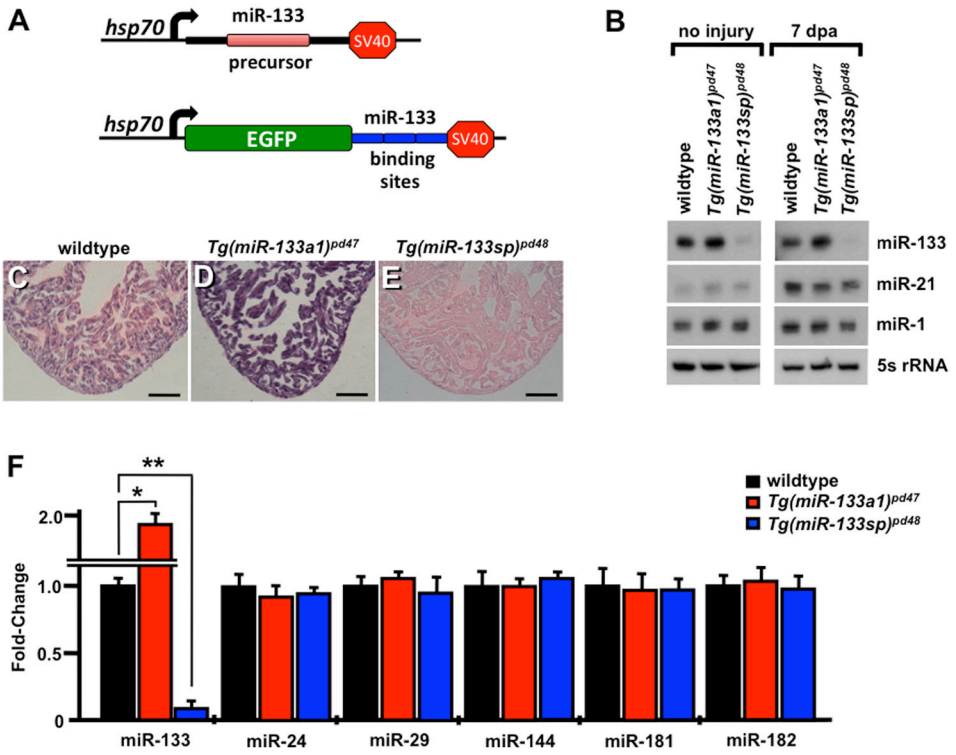

Fig. 2.

Inducible transgenic strains modulate miR-133 expression *in vivo*. A) Transgenic constructs for inducible overexpression (*Tg(miR-133a1)*^{pd47}; top) or reduction of miR-133 *(Tg(miR-133sp)*^{pd48}; bottom). B) Northern blot analyses demonstrating elevated miR-133 levels in *Tg(miR-133a1)*^{pd47} ventricles, and miR-133 depletion in *Tg(miR-133sp)*^{pd48} samples, following heat induction (uninjured, left; 7 dpa, right). No differences were detected in mature miR-21 and miR-1 levels among wildtype, *Tg(miR-133a1)*^{pd47} and *Tg(miR-133sp)*^{pd48} samples. *5s* rRNA was used as a control for Northern blot studies. C–E) *In situ* hybridizations reveal levels of miR-133 remain elevated in *Tg(miR-133a1)*^{pd47} and diminished in *Tg(miR-133sp)*^{pd48} 24 hours after the completion of heat-treatment, when compared to heat-treated wildtype controls. F) Real-time QPCR studies document miR-133 levels are significantly elevated in *Tg(miR-133a1)*^{pd47} and depleted in *Tg(miR-133sp)*^{pd48} heart samples. Expression of miR-24, miR-29, miR-144, miR-181 and miR-182 are unaltered under conditions of miR-133 modulation. Student's t-test p-value <0.05 for * and **. (sp, sponge; dpa, days post-amputation). Scale bar in (C–E) represents 100 μm.

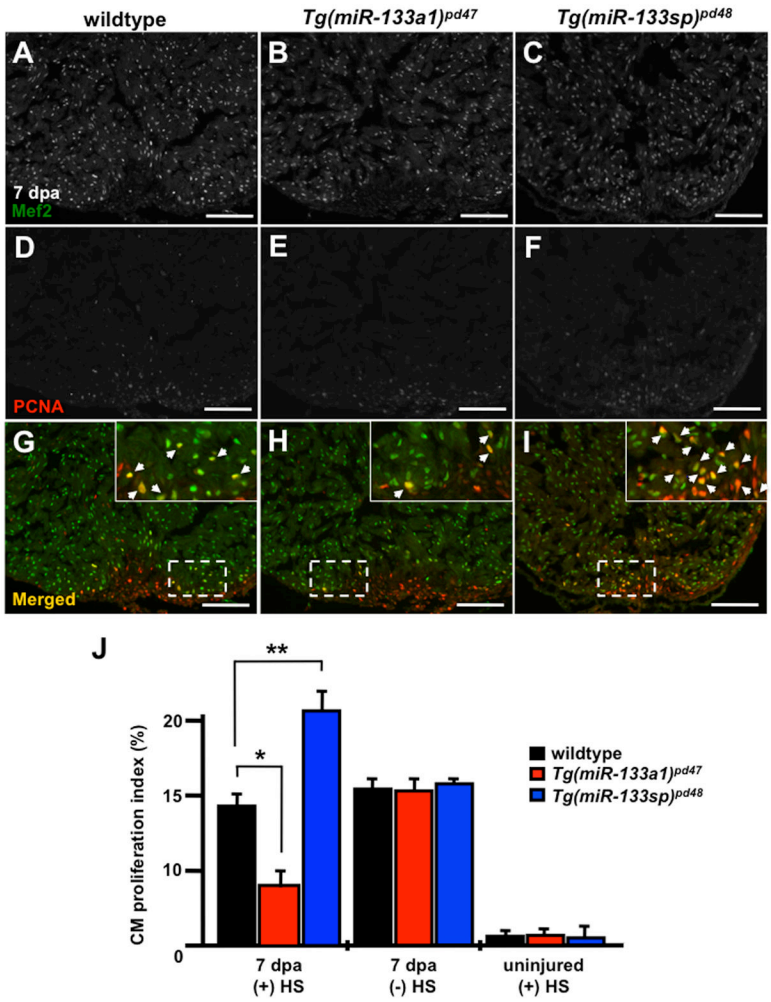

Fig. 3.

miR-133 restricts cardiomyocyte proliferation during heart regeneration. A–I) Wildtype, *Tg(miR-133a1)*^{pd47} and *Tg(miR-133sp)*^{pd48} adult hearts were resected, allowed to regenerate for 6 days, and subjected to a single heat-treatment at 38°C. Representative 7 dpa wildtype, *Tg(miR-133a1)*^{pd47} and *Tg(miR-133sp)*^{pd48} heart sections were stained with Mef2 (A–C) and PCNA (D–F) and subsequently merged (G–I). Inserts in (G–I), high zoom images of the white dashed rectangle; arrowheads indicate proliferating CMs. J) CM proliferation indices were determined for each group at 7 dpa. n = 10 – 12; Mean ± SEM, Student's t-test p-value <0.001 for * and **. HS = heat-shock. Scale bar in (A–I) represents 100 μm.

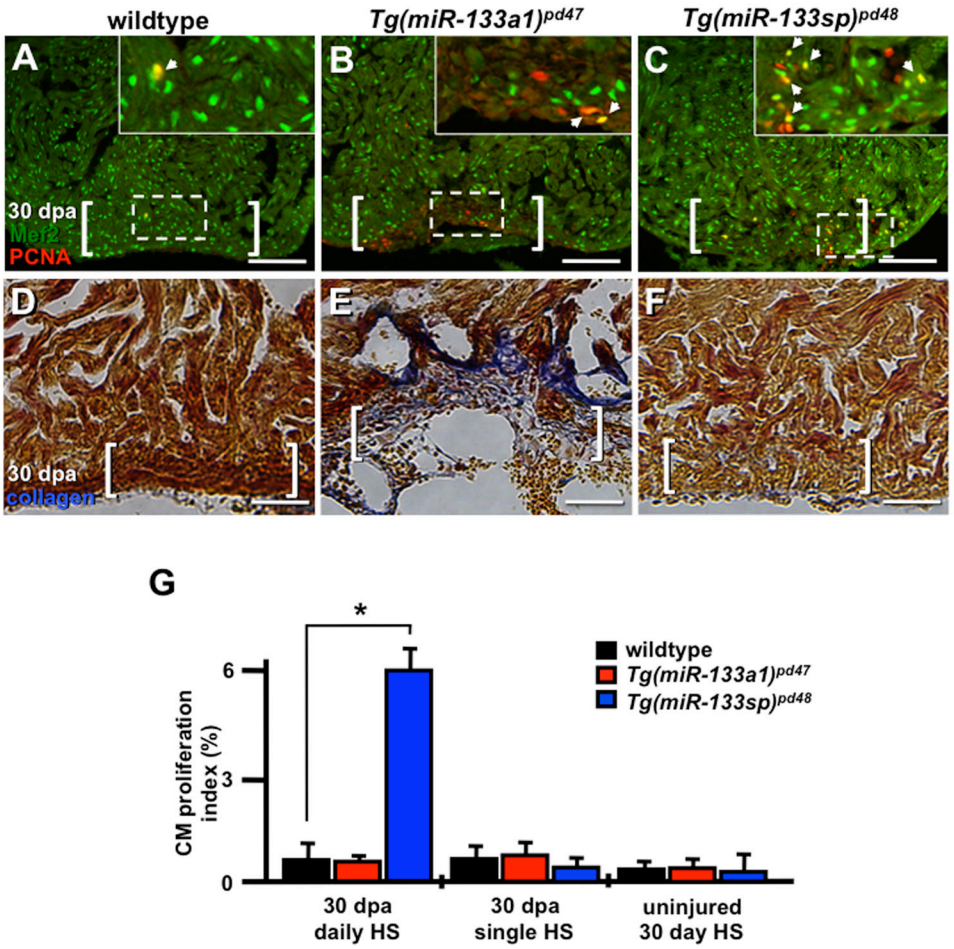

Fig. 4.

Sustained miR-133 expression is associated with scar formation. A–F) Wildtype, *Tg(miR-133a1)*^{pd47} and *Tg(miR-133sp)*^{pd48} adult hearts were resected and subjected to daily heat-treatment at 38°C for 30 days. A–C) Representative 30 dpa wildtype, *Tg(miR-133a1)*^{pd47} and *Tg(miR-133sp)*^{pd48} heart sections were stained with Mef2 (green) and PCNA (red). Inserts in (AC), high zoom images of the white dashed rectangle; arrowheads indicate proliferating CMs. D–F) Alternatively, representative 30 dpa wildtype control, *Tg(miR-133a1)*^{pd47} and *Tg(miR-133sp)*^{pd48} adult hearts sections stained to detect Collagen with an AFOG assay. G) CM proliferation indices were determined for each group at 7 dpa. n = 8 – 12; Mean ± SEM, Student's t-test p-value <0.001 for * and **. HS = heat-shock. Scale bar in (A–F) represents 100μm. White brackets represent approximate amputation planes. HS = heat-shock. AFOG = acid fuchsin orange G.

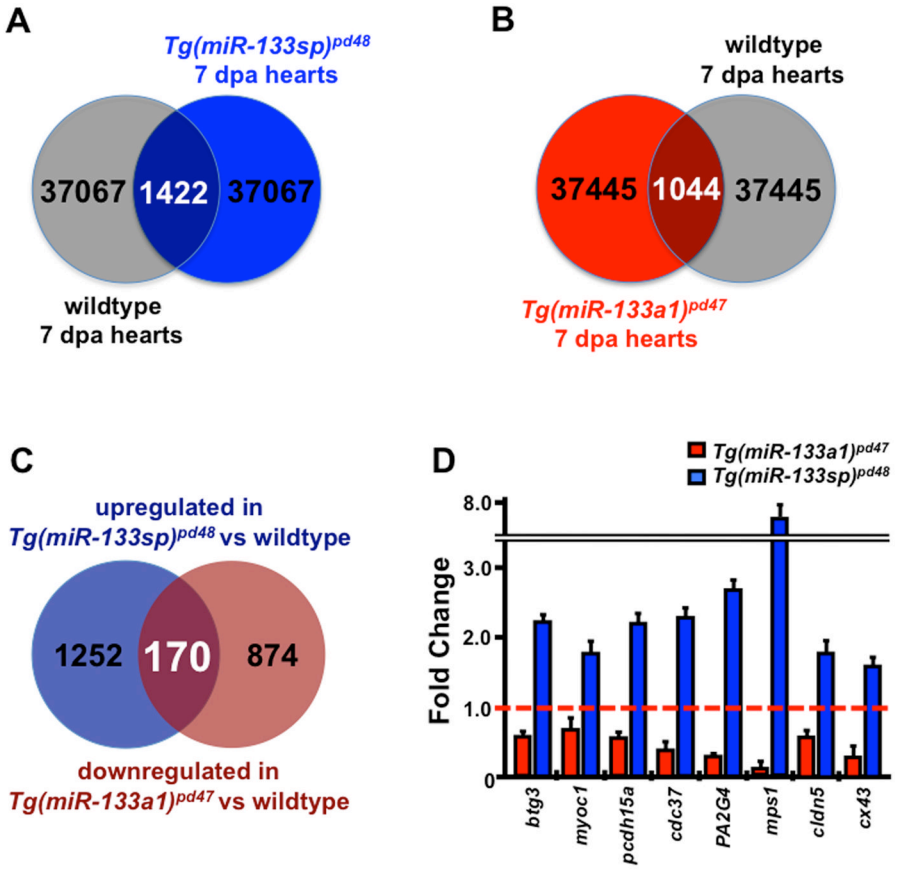

Fig. 5.

miR-133 regulates cell cycle and junction proteins during heart regeneration. A–C) Summary of mRNA microarray results. 1422 genes were upregulated in 7 dpa *Tg(miR-133sp)*^{pd48} samples (versus wildtype) (A), and 1044 genes were downregulated in 7 dpa *Tg(miR-133a1)*^{pd47} samples (versus wildtype) (B). The overlap of 170 genes contained in each group is likely enriched for miR-133 targets (C). D) Real-time Q-PCR analysis of candidate miR-133 target genes in 7 dpa hearts, from triplicate experiments. Under conditions of elevated miR-133 levels, *Tg(miR-133a1)*^{pd47}, potential target genes were detected at lower levels. Conversely, in *Tg(miR-133sp)*^{pd48} hearts, these genes were elevated by comparison with wildtype controls. *btg3, B-cell translocation gene 3; cldn5, claudin-5; myoc1, myosin IC; pcdh15a, protocadherin 15a; cdc37, cell division cycle 37; PA2G4, proliferation associated protein; mps1, cell cycle kinase; cx43*, connexin-43.

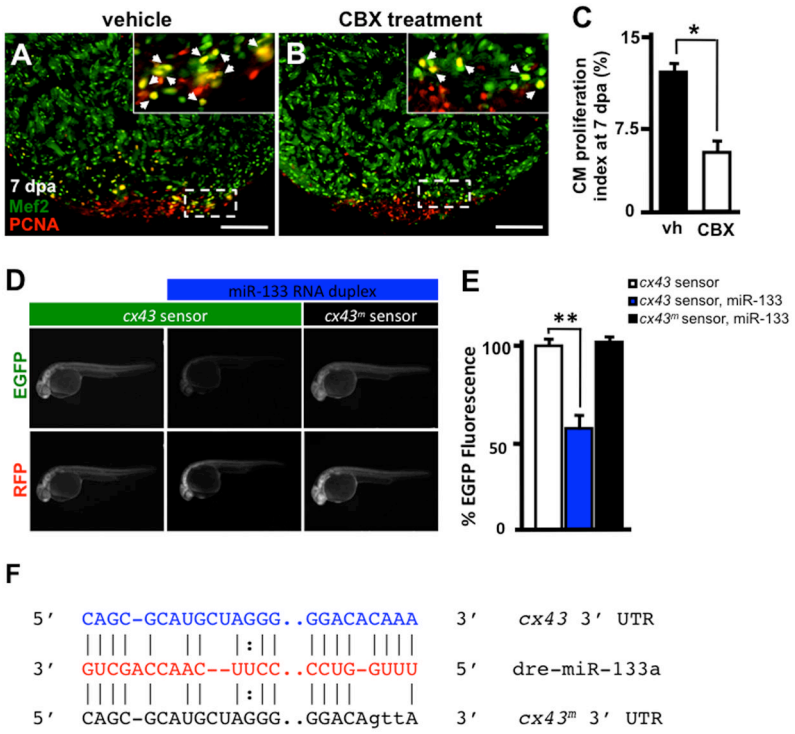

Fig. 6.

miR-133 regulates *cx43 in vivo*. A–B) Wildtype *Ekkwill* ventricles were resected and allowed to regenerate for 6 days prior to incubation with either vehicle or 50μM CBX for 24 hrs. Representative vehicle (vh) and carbenoxolone-treated (CBX) 7 dpa heart sections stained with Mef2 (green) and PCNA (red). Insets in (A, B), high-zoom images of the white dashed rectangle; arrowheads indicate proliferating CMs. C) CM proliferation indices were calculated for each group at 7 dpa. D) Embryos were injected with *EGFP-cx43* sensor and *mCherry* mRNA in the absence (left column) or presence (middle column) of miR-133 RNA duplex. A mutated *EGFP-cx43* sensor was also co-injected with miR-133 RNA duplex (right column). E) Quantification of EGFP fluorescence was determined at 24 hpf. F) Alignment of putative miR-133 binding sites in the 3' UTR of *cx43*. Predictions were based on the Microcosm database. Three point mutations were introduced in the *cx43* miR-133 binding site. n = 10–12; Mean ± SEM, Student's t-test p-value <0.01 for * and **. hpf = hours post-fertilization. Scale bar in (A–B) represents 100 μm.